

Measuring $|V_{td}|$ at the LHCEzequiel Alvarez,^{1,*} Leandro Da Rold,^{2,†} Mariel Estevez,^{1,‡} and Jernej F. Kamenik^{3,4,§}¹*International Center for Advanced Studies (ICAS) and CONICET, UNSAM,
Campus Miguelete 25 de Mayo y Francia, 1650 Buenos Aires, Argentina*²*Centro Atómico Bariloche, Instituto Balseiro and CONICET Av. Bustillo 9500,
8400 S. C. de Bariloche, Argentina*³*Jožef Stefan Institute, Jamova 39, 1000 Ljubljana, Slovenia*⁴*Faculty of Mathematics and Physics, University of Ljubljana,
Jadranska 19, 1000 Ljubljana, Slovenia*

(Received 26 November 2017; published 12 February 2018)

We propose a direct measurement of the Cabibbo-Kobayashi-Maskawa element V_{td} at the LHC. Making use of the imbalance between d and \bar{d} quark content in the proton, we show that a nonzero V_{td} induces a charge asymmetry in the tW associated production. The main backgrounds to this process— $t\bar{t}$ production, and tW -associated production mediated by V_{tb} —give charge-symmetric contributions at leading order in QCD. Therefore, using specific kinematic features of the signal, we construct a charge asymmetry in the dilepton final state which—due also to a reduction of systematic uncertainties in the asymmetry—is potentially sensitive to V_{td} suppressed effects. In particular, using signal and background simulations up to the detector level, we show that this new observable could already improve the current direct upper bound on $|V_{td}|$ with existing LHC data. We also project that $|V_{td}|$ values down to ~ 10 times the standard model prediction could be probed at the high-luminosity LHC.

DOI: 10.1103/PhysRevD.97.033002

I. INTRODUCTION

The entries in the Cabibbo-Kobayashi-Maskawa (CKM) matrix governing flavor transitions among quarks are fundamental parameters of the standard model (SM). As such, they warrant intense experimental scrutiny. Currently, the first two rows of the CKM matrix are already being probed directly with ever improving precision using decays of nuclei, kaons, charmed mesons, and B hadrons [1–8]. On the other hand, few direct experimental techniques exist regarding the third row of the CKM matrix [1,9]. The SM predictions for V_{tq} matrix elements (with $q = d, s, b$) are currently derived from CKM unitarity considerations, as well as measurements of radiative decays and oscillations of B mesons, where V_{tq} enter in loops involving virtual top quarks. A recent global CKM fit yielded [10]

$$\begin{aligned} |V_{tb}^{\text{SM}}| &= 1 - 8.81_{-0.24}^{+0.12} \times 10^{-3}, \\ |V_{ts}^{\text{SM}}| &= 41.08_{-5.7}^{+3.0} \times 10^{-3}, \\ |V_{td}^{\text{SM}}| &= 8.575_{-0.098}^{+0.076} \times 10^{-3}. \end{aligned} \quad (1)$$

The assumptions of CKM unitarity and the dominance of SM contributions in loop-suppressed rare flavor processes, which allow for the precise third row CKM moduli determinations above, are in general not valid once one considers physics beyond the SM (see, e.g., Ref. [11]). One possibility to approach such scenarios is to consider the mass decoupling limit, where the dominant new physics (NP) effects are captured by the SM effective field theory (SMEFT) [12,13]. Unfortunately, a completely general model-independent analysis of constraints on Wtd_i interactions within the SMEFT framework has not yet been performed, and we can at present only relate to studies in more specific NP frameworks. For example, a comprehensive analysis of direct and indirect constraints on the Wtd_i (as well as Ztu_i and Htu_i) interactions in models of heavy vector-like quarks [14] found that the strongest constraints on the Wtd_i couplings in such scenarios actually come from studies of top-quark decays.

The aim is thus to confront the SM predictions of $|V_{tq}|$ (as determined from indirect probes) using direct measurements of processes involving on-shell top quarks. The LHC, as currently the only top-quark production machine,

*sequi@df.uba.ar
†daroldl@cab.cnea.gov.ar
‡mestevez@unsam.edu.ar
§jernej.kamenik@ijs.si

Published by the American Physical Society under the terms of the Creative Commons Attribution 4.0 International license. Further distribution of this work must maintain attribution to the author(s) and the published article's title, journal citation, and DOI. Funded by SCOAP³.

can probe V_{tq} directly by studying top production as well as decays. In particular, measurements of b -jet fractions in top decays $t \rightarrow Wj$ currently put a bound on [15]

$$\frac{\mathcal{B}(t \rightarrow bW)}{\sum_{q=d,s,b} \mathcal{B}(t \rightarrow qW)} > 0.955 @ 95\% \text{C.L.}, \quad (2)$$

which can be interpreted as $\sqrt{|V_{td}|^2 + |V_{ts}|^2} < 0.217|V_{tb}|$. In addition, precise measurements of t -channel single top production and its charge asymmetry at the LHC [16–18] when compared with the accurate theoretical predictions [19–22] can be interpreted as measurements of $|V_{tq}|$. A recent ATLAS analysis neglecting $|V_{td,ts}|$ effects yielded $|V_{tb}| = 1.07 \pm 0.09$ [16]. While such measurements are in principle also able to probe the $|V_{ts}|$ and $|V_{td}|$ matrix elements [23,24], they are intrinsically limited by the overwhelming backgrounds and associated statistical and systematic uncertainties. Consequently, especially in the case of $|V_{td}|$ they are not expected to come even close to the magnitude of the SM predictions.

In the present work we outline an experimental strategy to probe the $|V_{td}|$ matrix element directly at the LHC using single top production associated with a W boson ($pp \rightarrow tW$).¹ Our proposal exploits the production cross-section enhancement as well as boosts of the top quarks coming from initial-state valence d partons. In addition, and contrary to t -channel single top production, the main backgrounds have vanishing or very small charge asymmetries. This opens a path towards direct $|V_{td}|$ determination at the high-luminosity (HL) LHC within an order of magnitude of the SM prediction.

The remainder of the paper is structured as follows. In Sec. II we review the main effects of a nonvanishing V_{td} on top-quark production processes at hadron colliders. In Sec. III we focus on the charge asymmetry in Wt production by analyzing the dominant backgrounds and proposing an analysis strategy to reduce these while preserving most of the signal. The main results of this work are presented in Sec. IV, and we present our conclusions in Sec. V.

II. LHC PROCESSES AND OBSERVABLES SENSITIVE TO V_{td}

The production of the top quark from an initial down quark in the proton is highly suppressed because of the expected smallness of $|V_{td}| \sim \mathcal{O}(10^{-2})$. Any relevant process mediated via the tWd coupling is expected to produce a tiny signal, and thus would be difficult to measure directly at the LHC, both because of the small expected statistics and large backgrounds, but especially because of systematic uncertainties inherent to a hadronic machine. Therefore, the

¹For a previous study of possible NP effects in this mode, see Ref. [25].

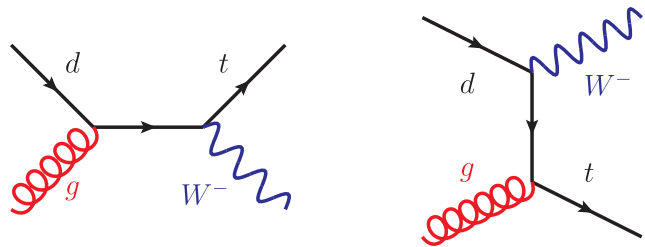


FIG. 1. Feynman diagrams contributing to $pp \rightarrow tW$ production proportional to V_{td} at LO in QCD.

observability of V_{td} -sensitive processes at the LHC is closely related to the capability of finding associated observables with reduced experimental systematic uncertainties. Common approaches to taming systematics include data-driven methods and asymmetries. Since the d quark is a valence constituent of the proton, its imbalance with the \bar{d} quark together with the charge self-tagging of leptonically decaying W bosons and top quarks motivates us to explore V_{td} -sensitive observables in the form of charge asymmetries. In the following we will parametrize eventual departures from SM in V_{td} through the ratio

$$r \equiv \left| \frac{V_{td}}{V_{td}^{\text{SM}}} \right| \quad (3)$$

in order to classify processes according to their leading power in r .

As a first process, we discuss the tW -associated production mediated by the partonic process $gd \rightarrow tW^-$ [see Fig. 1 for the relevant leading order (LO) Feynman diagrams], whose cross section is proportional to $|V_{td}|^2$ (and thus r^2). At LO in the SM $\sigma(tW^-) = 20$ fb [26] at the 13 TeV LHC, while for the CP -conjugate final state $\sigma(\bar{t}W^+) = 6$ fb. This process is interesting because of both its sizable charge asymmetry and that its kinematics predicts a characteristic angular distribution. In fact, the dominant diagram has a virtual top quark exchanged in the t channel. Because of the relatively large incoming momentum expected on average from a valence d quark, it consequently prefers a forward W^- in the lab frame. This special feature allows to consider the interesting dilepton final state, which permits a relatively clean search strategy. In fact, this forward preference of the W^- translates to having a preferably forward ℓ^- in signal events. The two main backgrounds to this $\ell^+ \ell^- b p_T^{\text{miss}}$ final state would be the dileptonic $t\bar{t}$ production (missing one of the b jets from top decays) and tW -associated production proportional to $|V_{tb}|^2$ (also in the leptonic decay channel of both the t and the W). Since this process features a collinear b coming from initial-state gluon splitting [either resummed as in the five-flavor parton distribution function (PDF) scheme, or explicit as in the four-flavor PDF scheme], in the following we denote it as $tW(b)$ production. Importantly, both backgrounds have very small charge asymmetries, and we expect

a charge asymmetry constructed with this final state to exhibit promising sensitivity to V_{td} . Other reducible backgrounds and their relevance are discussed in more detail in the next section.

Another potentially important V_{td} -sensitive process is $pp \rightarrow tj$, where partonic processes such as $dq \rightarrow tq'$ and $d\bar{q}' \rightarrow t\bar{q}$ yield contributions that go as $|V_{td}|^2$; see Fig. 2. (Here, $q = u, c$ and $q' = d, s, b$.) This process has a contribution where both initial quarks are valence quarks, $du \rightarrow td$, and therefore it is enhanced with respect to the contribution of its CP conjugate, producing a charge asymmetry. However, its main background—the t -channel single top production [$pp \rightarrow tj(b)$] proportional to $|V_{tb}|^2$ —is also significantly charge asymmetric. The sensitivity in this channel is thus limited by both the theoretical knowledge of its SM prediction and experimental systematics in its measurement, and we do not pursue it further.

So far we have discussed signals whose cross sections are proportional to $|V_{td}|^2$ (r^2). However, one could also consider (tree-level) processes contributing at higher orders in V_{td} . For instance, the contribution to WW production coming from $d\bar{d} \rightarrow W^+W^-$ with a top quark exchanged in the t channel is asymmetric in the angular distribution of the final-state particles and has a term proportional to $|V_{td}|^4$ (r^4). (See Fig. 2 for the relevant LO Feynman diagram on the right-hand side.) However, one of the main backgrounds to this signal would be the W^+W^- production mediated through the t -channel exchange of an up or charm quark, which has a similar asymmetry as the signal. Again, in this case the usefulness of the asymmetry is reduced because one would need to compare it to a non-negligible reference number of the background. However, there are two features of this process that should be mentioned and which may deserve further exploration. One is that its cross section has a term proportional to r^4 , and although this contribution is suppressed by V_{td}^4 , it is doubly enhanced compared to previous ones for $r > 1$. The second feature is that this process would affect both the angular and invariant mass distributions of the WW final state, and a sensitive observable could be constructed using sideband fitting.

There exist further V_{td} -sensitive processes which we do not discuss here. Instead, in the remainder of the paper we focus on $pp \rightarrow tW$ and study the prospects of measuring or

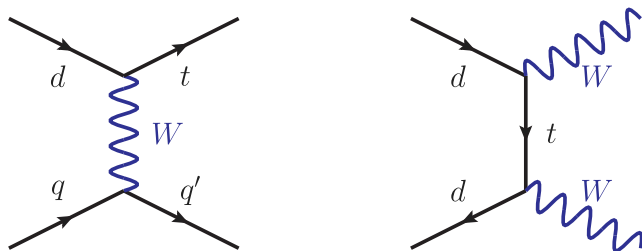


FIG. 2. Examples of Feynman diagrams contributing to further V_{td} -sensitive processes at the LHC.

constraining V_{td} through a suitably defined charge asymmetry in the dilepton final-state channel.

III. ASYMMETRY SENSITIVE TO V_{td}

In this section we explore potential direct experimental sensitivity to V_{td} through the process $pp \rightarrow tW$ at the LHC. As discussed in the previous section, the kinematics of the signal offers the opportunity to distinguish the leptons coming from the W and the top decay, and therefore allows for a search strategy using a charge asymmetry in the $\ell^+\ell^-bP_T^{\text{miss}}$ final state. In the following subsections we first analyze the relevant backgrounds before constructing a suitable V_{td} -sensitive charge asymmetry. We end by discussing other charge asymmetries which could provide further valuable observables in other contexts.

A. Backgrounds

In the following we discuss the main backgrounds and give an estimate of their size. The actual numbers used in our results are obtained through simulations described in the next section. We first note that the ATLAS and CMS collaborations have analyzed this process in both 8 and 13 TeV LHC data [27–29]. Here we roughly follow Ref. [27] in the detailed characterization of the backgrounds, considering the final state with two leptons and a b jet. We start by discussing the main backgrounds first.

The $t\bar{t}$ production in the fully leptonic channel with a missed b jet leads to the same final state as the signal. Being produced by QCD interactions, this is the dominant background, with a LO cross section of order $\sigma(t\bar{t}) \sim 500$ pb and at next-to-leading order (NLO) $\sigma(t\bar{t}) \sim 680$ pb (both estimated through `MadGraph5_aMC@NLO` [26]). Requiring exactly one b jet within the typical detector acceptance [$|\eta_b| < 2.5$ and $p_T(b) > 20$ GeV] and no other jet with $|\eta| < 5$ and $p_T > 20$ GeV leads to a considerable reduction of this background, suppressing it by a factor $\sim 10^{-2}$ at the parton level. At LO, $t\bar{t}$ arises from gluon fusion or from $q\bar{q}$ with a gluon in an s channel, and so is completely charge symmetric. However, having a large cross section, it suppresses any net charge asymmetry by contributing to its denominator. At NLO this background does give a small asymmetric contribution, with its size depending on the specific definition of the charge asymmetry, as described in the next section.

Another important background is given by the $tW^-(\bar{b})$ and $\bar{t}W^+(b)$ final states, without intermediate on-shell t or \bar{t} .² The LO production cross section is $\sigma(tW(b)) \sim 28$ pb [26]. At NLO this background is expected to develop a small charge asymmetry, but since its cross section is

²In a four-flavor PDF scheme, this background is dominated by gluon fusion similar to $t\bar{t}$, whereas in the five-flavor PDF scheme the LO partonic process is $gb \rightarrow tW$ and the final state matches the signal exactly. See, e.g., Ref. [30] for details on separating this process from $t\bar{t}$ production in simulations.

considerably smaller than $t\bar{t}$, in practice we can safely neglect it.

The Drell-Yan-dominated $\ell^+\ell^-j$ production, with j misidentified as a b jet, is in principle an important background. Since the lepton pair arises from an intermediate Z or γ , ℓ^+ and ℓ^- have the same flavor. The LO cross section is of the order $\sigma(\ell\ell j) \sim 440$ pb. The presence of the jet induces a charge-asymmetric distribution. This background can be drastically reduced by demanding different flavors of the final-state leptons at the expense of losing half of the signal. A significant reduction is instead obtained by demanding $m_{\ell\ell}$ larger than 25 GeV and excluding a region around the Z mass, which we choose between 75 and 105 GeV. Besides, since the signal has missing energy from the undetected neutrino arising from the leptonic decay of the top and W , whereas there is no missing energy for this background, we demand $E_T^{\text{miss}} > 30$ GeV. These cuts, in addition to a rejection factor of mistagging the light jet as a b , make the final contribution of this background to the cross section negligible.

There is also a background similar to the previous one, but with a $b\bar{b}$ pair in the final state: $\ell^+\ell^-b\bar{b}$. The LO cross section is of the order $\sigma(\ell\ell b) \sim 32$ pb, but cuts in $m_{\ell\ell}$ and E_T^{miss} reduce this background as in the case of $\ell^+\ell^-j$. Although in the present case there is no significant rejection factor associated with the jet(s), the asymmetry in $\ell^+\ell^-b$ is much smaller than that of $\ell^+\ell^-j$, as can be expected since the b quark is not a valence quark.

The t -channel single top production [$tj(b)$ and $\bar{t}j(b)$], with the j misidentified as a lepton, gives a large asymmetric background: $\sigma(tj(b)) \simeq 52$ pb and $\sigma(\bar{t}j(b)) \simeq 35$ pb, at LO. A lepton misidentification rate of the order $\sim 10^{-4}$ [31] suppresses this background, leading to a negligible cross section.

Other backgrounds include WWj , with j being either a light or heavy (b or c) jet flavor. The first case has a sizable charge asymmetry, although a large rejection factor. The second case has a small rejection factor, but a tiny charge asymmetry. We have verified that both of these backgrounds are unimportant.

We note that some of the backgrounds listed above have contributions that depend on V_{td} , and could be enhanced for $r > 1$. However, even for $r \sim \mathcal{O}(10)$, the size of the backgrounds does not change significantly. In particular, the $t\bar{t}$ production is overwhelmingly dominated by QCD interactions, so an increase of the very small V_{td} by a factor $\mathcal{O}(10)$ has no discernible effect on this background. For the backgrounds $\ell\ell j$ and $\ell\ell b$, the dilepton pair arises from an intermediate Z or γ^* , and thus they are independent of V_{td} at LO. The t -channel single top background, on the other hand, includes contributions sensitive to V_{td} already at LO, but they are again very small for $|V_{td}| \lesssim \mathcal{O}(10^{-1})$. As an example, for $r = 10$ ($r = 20$) the production cross section increases by 5% (20%). Therefore, for moderate values of r this background does not have a significant growth. For WWj , there

are Feynman diagrams depending on V_{td} ; however, similar to the case of $t\bar{t}$, their contribution is tiny compared to the dominant contributions that are proportional to the diagonal elements of the CKM matrix. Thus, even for $r \sim \mathcal{O}(10)$ the impact on this background can be neglected.

At last, it should be mentioned that the partonic initial states gs and $g\bar{s}$ can generate an irreducible background controlled by V_{ts} , namely, $gs \rightarrow tW$. However, this background has a cross section suppressed by both the smallness of $|V_{ts}|$ and the strange-quark PDF, plus a negligible charge asymmetry, and therefore we can safely neglect it even for values of $|V_{ts}|$ at the current experimental upper bound.

Since the signal results in a $\ell^+\ell^-b p_T^{\text{miss}}$ final state, we enhance our signal over the main backgrounds $tW(b)$ and $t\bar{t}$ by requiring in the latter that only one of the b 's falls into the acceptance region defined by $|\eta(b_1)| < 2.5$ and $p_T(b_1) > 20$ GeV, while the second b is restricted to the regions $|\eta(b_2)| > 5$ or $p_T(b_2) < 20$ GeV, mimicking a jet-veto aimed predominantly at suppressing the $t\bar{t}$ background (more sophisticated methods for dealing with this overwhelming background are discussed in the next sections).

We therefore find that main backgrounds are suppressed through the following selection of events:

- (1) Basic cut: Select events with $\ell^+\ell^-b$, all with $|\eta| < 2.5$ and $p_T > 20$ GeV.
- (2) $t\bar{t}$ suppression cut: Veto events with additional jets within $|\eta| < 5$.
- (3) Z/γ^*j suppression cut: Veto events with $E_T^{\text{miss}} < 30$ GeV, $m_{\ell\ell} < 25$ GeV, or $|m_{\ell\ell} - m_Z| < 15$ GeV.

In Table I we show how signal and main backgrounds are affected by these selection cuts.

B. Enhancing a charge-asymmetric signal over a (mostly) symmetric background

Given the above discussion we are left with a charge-asymmetric signal in $pp \rightarrow tW$, and the approximately symmetric main backgrounds $pp \rightarrow t\bar{t}$ and $pp \rightarrow tW(b)$.

TABLE I. Cut flow for the signal process and for the main backgrounds $t\bar{t}$ and $tW(b)$ at the parton level as described in the text. Each column adds a new cut to the previous columns. As it can be seen, this selection of events is not enough to emerge signal over the backgrounds; this is achieved in the next paragraphs when we construct an asymmetry that makes use of the different distributions in signal and backgrounds. Simulation details are described in Sec. IV.

Process	$\sigma \cdot \mathcal{B}$ [fb]	Basic [fb]	$t\bar{t}$ suppression [fb]	Z/γ^*j suppression [fb]
Signal	$1.2r^2$	$0.59r^2$	$0.53r^2$	$0.35r^2$
$t\bar{t}$	3.1×10^4	3.4×10^3	1.4×10^3	9.6×10^2
$tW(b)$	1.8×10^3	7.4×10^2	6.3×10^2	4.1×10^2

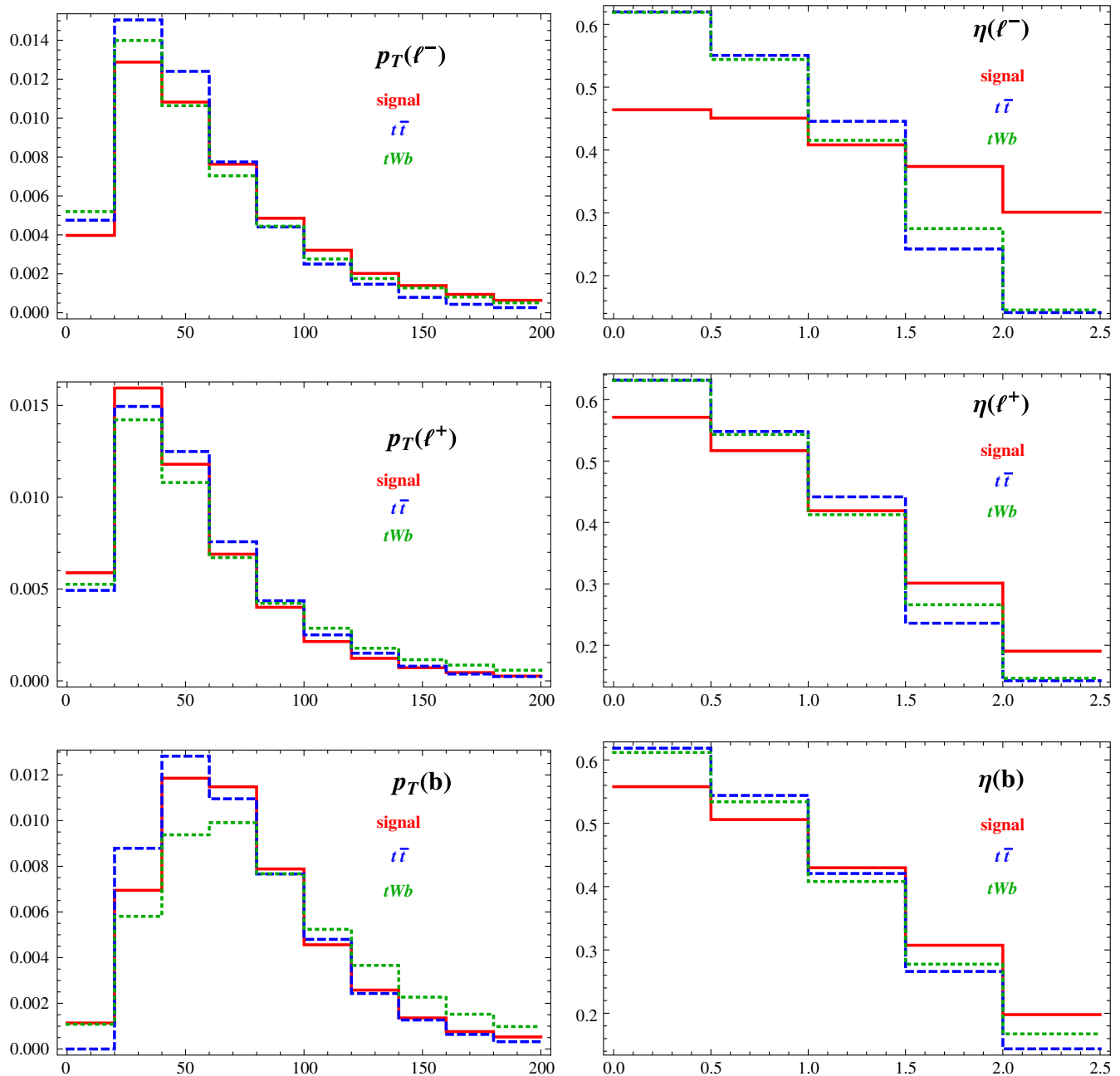


FIG. 3. Distributions of p_T and η of the final particles at the parton level for the LO signal (red solid line) and the main backgrounds NLO $t\bar{t}$ (blue dashed line) and LO $tW(b)$ (green dotted line). Each sample contains the corresponding process and its charge conjugate, since on an event-by-event basis one cannot distinguish which lepton comes from the t decay and which from the associatively produced W decay.

Other backgrounds are negligible or become negligible after a cut in E_T^{miss} and $m_{\ell\ell}$, such as $pp \rightarrow Z/\gamma^* j$.

In order to quantify the different signal and background features expected from the previous analysis, we first consider the relevant distributions of the signal and the main backgrounds. For this purpose, we have simulated at the parton level signal and $tW(b)$ at LO and $t\bar{t}$ at NLO, as explained in Sec. IV. The $tW(b)$ background has been simulated in the four-flavor PDF scheme with

$m_b = 4.7$ GeV, resulting in a tWb final state.³ The results are shown Fig. 3. We observe that the most important difference comes from the $\eta(\ell^-)$ distribution, where the signal clearly prefers forward negatively charged leptons, as expected from the qualitative discussion in Sec. II.

³See Ref. [32] for a discussion on the appropriate use of this scheme.

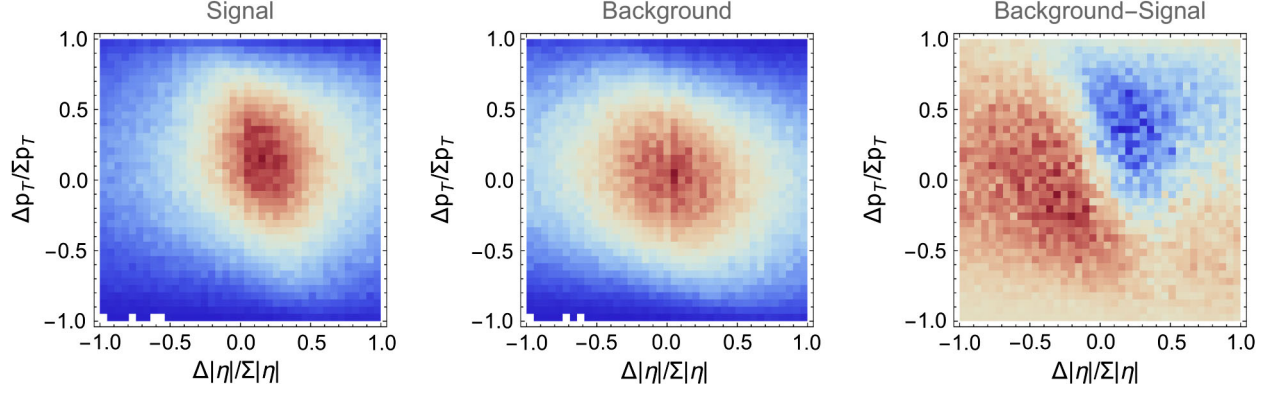


FIG. 4. Density plot of normalized event distributions of the signal (left) and the main background $t\bar{t}$ (center) in the $\Delta|\eta(\ell)|/\Sigma|\eta(\ell)|$ versus $\Delta p_T(\ell)/\Sigma p_T(\ell)$ plane. In the right panel we show the difference between the two distributions, which demonstrates that (compared to the almost symmetric background) signal events are predominantly in the third quadrant of the plot, whereas they are missing in the first quadrant. This correlation between the plotted variables points out that an asymmetry between these quadrants would be useful to enhance signal over background.

A similar preference is also present in the $\eta(\ell^+)$ and $\eta(b)$ distributions, although much less pronounced. On the other hand, the p_T distributions of the signal and the backgrounds do not offer as clear a differentiation as in the η case. For example, the $p_T(b)$ [$p_T(\ell^-)$] distributions could only be used to distinguish the signal from $tW(b)$ ($t\bar{t}$), respectively.

Given these distinctions between the signal and backgrounds in one-variable distributions, we next study distributions of pairs of variables in order to construct the most sensitive observables that could enhance the signal over the background. With this purpose, and motivated by the results in Fig. 3, we plot in Fig. 4 the simultaneous (normalized) distributions of the signal and the main ($t\bar{t}$) background in the $\Delta|\eta(\ell)|/\Sigma|\eta(\ell)|$ — $\Delta p_T(\ell)/\Sigma p_T(\ell)$ plane, where

$$\begin{aligned}\Delta|\eta(\ell)| &= |\eta(\ell^+)| - |\eta(\ell^-)|, \\ \Sigma|\eta(\ell)| &= |\eta(\ell^+)| + |\eta(\ell^-)|, \\ \Delta p_T(\ell) &= p_T(\ell^+) - p_T(\ell^-), \\ \Sigma p_T(\ell) &= p_T(\ell^+) + p_T(\ell^-).\end{aligned}\quad (4)$$

As it can be seen in the figure, a sizable asymmetry in the signal can be constructed by comparing events in the first and third quadrants. Thus, we propose the asymmetry

$$A(\eta, p_T) = \frac{N^+ - N^-}{N^+ + N^-}, \quad (5)$$

where

$$N^\pm = N(\Delta|\eta(\ell)| \gtrless 0 \ \& \ \Delta p_T(\ell) \gtrless 0), \quad (6)$$

as a $|V_{id}|$ sensitive observable.

It is interesting to understand how the different processes contribute in $A(\eta, p_T)$. It is clear that the denominator is

dominated by $t\bar{t}$, whose cross section is considerably larger than the others, even after the selection cuts. On the other hand, the numerator is more involved because each i th process contributes with

$$N_i^+ - N_i^- = \sigma_i \cdot \mathcal{A}_i \cdot \epsilon_i \cdot A_i(\eta, p_T), \quad (7)$$

where the factors on the rhs are the cross section, acceptance, selection efficiency,⁴ and asymmetry, respectively, all restricted exclusively to the i th process. Since $t\bar{t}$ has a small NLO charge asymmetry, but a large cross section, it ends up being important for the $r \approx 1$ region, but becomes subleading as $r \gtrsim 10$. We expect a similar NLO asymmetry for $tW(b)$, but since its cross section is much smaller than $t\bar{t}$ we can neglect it in the numerator. Other backgrounds such as WWj , tj , and Z/γ^*j have a non-negligible asymmetry, but their product $\sigma_i \cdot \mathcal{A}_i \cdot \epsilon_i$ suppresses any contribution to the numerator.

C. Other asymmetries

Given the distributions in Fig. 3 one could consider alternative definitions of asymmetries to enhance the signal over the backgrounds. We have tested many of them bearing in mind that we need to exploit the lepton charge asymmetry present in the signal. In the following paragraphs, we explain the main ones and why they do not improve the significance of the asymmetry defined in Eq. (5).

The most interesting attempt consists of taking the asymmetry $A(\eta, p_T)$ with a cut in $|\eta_{\ell^-}| \gtrsim 1.5$ since we expect to have an enhanced asymmetry in the forward region. Indeed, this selection increases the absolute value of

⁴Selection efficiency refers to the fraction of events that pass the selection cuts to be either N^\pm .

TABLE II. The relevant processes upon detector acceptance and selection cuts. \mathcal{A} refers to the detector acceptance of $\ell^+\ell^-b$ plus anything else. The selection efficiency ϵ includes a veto on events with extra jets, cuts in E_T^{miss} and $m_{\ell\ell}$, and also a selection of events only in the first and third quadrants in $\Delta|\eta|$ and Δp_T , as defined in Eq. (6). The column labeled “ $\sigma \cdot \mathcal{B} \cdot \mathcal{A} \cdot \epsilon$ ” is relevant for the denominator of the total asymmetry and is dominated by $t\bar{t}$ and a small correction by $tW(b)$. A_i refers to the asymmetry defined in Eq. (5) for the corresponding row, constructed with the detector-level events that pass all acceptance and selection requirements. Finally, the last column is relevant for the numerator of the total asymmetry and is dominated by $t\bar{t}$ for $r \lesssim 10$ and by the signal for $r \gtrsim 10$.

Process	$\sigma \cdot \mathcal{B}$ [fb]	$\mathcal{A}(\ell^+\ell^-b + X)$	ϵ	$\sigma \cdot \mathcal{B} \cdot \mathcal{A} \cdot \epsilon$ [fb]	$A_i(\Delta\eta , \Delta p_T)$	$\sigma \cdot \mathcal{B} \cdot \mathcal{A} \cdot \epsilon \cdot A_i$ [fb]
Signal	$1.2r^2$	0.17	0.16	$0.034r^2$	-0.2	$-0.0067r^2$
$t\bar{t}$	3.1×10^4	0.56	0.011	200	0.003	0.57
$tW(b)$	1.8×10^3	0.25	0.07	34	$\mathcal{O}(10^{-3})$	$\mathcal{O}(10^{-2})$
Z/γ^*j	5.1×10^5	0.002	4.7×10^{-4}	0.53	-0.10	-0.05
WWj	1.5×10^3	0.002	0.14	0.52	-0.06	-0.03
tj	1.7×10^4	1.2×10^{-5}	0.29	0.0062	-0.8	-0.02

the asymmetry, but reduces the acceptance due to the additional cut. Moreover, this also creates an artificial asymmetry in the backgrounds which reduces the sensitivity to the signal. Together, this results in larger statistical (and also presumed systematic) uncertainties and consequently reduced significance when compared to $A(\eta, p_T)$. On the other hand, imposing a symmetric cut on $|\eta_{\ell^-}|$ and $|\eta_{\ell^+}|$ keeps the backgrounds symmetric but does not increase the signal asymmetry sufficiently to offset the reduction in the acceptance.

The last case we discuss is the asymmetry based solely on $|\Delta\eta|$, with and without cuts on η , that is,

$$A(\eta) = \frac{N(\Delta|\eta(\ell)| > 0) - N(\Delta|\eta(\ell)| < 0)}{N(\Delta|\eta(\ell)| > 0) + N(\Delta|\eta(\ell)| < 0)}. \quad (8)$$

In this case the total number of accepted events increases and therefore the statistical uncertainty decreases. However, the absolute value of the asymmetry decreases because $\Delta|\eta|$ alone has less discriminating power than $\Delta|\eta|$ and Δp_T together (see the right panel in Fig. 4). The combination of these two features yields smaller significance than $A(\eta, p_T)$. While this asymmetry is also sensitive to cuts in η , we have found that their application does not improve the significance.

IV. RESULTS

For our quantitative analysis and estimation of the experimental reach, we have simulated the signal and the main backgrounds at the parton level using `madGraph5_aMC@NLO` [26]. The $t\bar{t}$ has been simulated at NLO in QCD to account for its nonvanishing charge asymmetry. The higher-order QCD effects in the other relevant processes have been accounted for through the effective k -factors. In particular, $k_{tW(b)} = 1.35$ [33] and we

assume the same k -factor for the signal.⁵ This exact procedure was used in the previous sections, where only parton-level results were utilized. For the results in this section we have in addition interfaced the parton-level simulation with `HERWIG` [35,36] (for $t\bar{t}$) and `PYTHIA8` [37,38] (for all other processes) for showering and hadronization. Finally, we have simulated detector effects using `DELPHES` [39]. The jets have been clustered using the anti- k_r algorithm with $R = 0.6$. A “loose” b -tagging algorithm working point has been used with a reference selection efficiency of 0.8 and a rejection factor for light jets of 100 [39,40]. The remaining `DELPHES` parameters have been left in the default ATLAS tune.

In all of the simulations we have used $m_t = 173$ GeV. We have used the `nn231o1` PDF for LO processes and the `nn23n1o` PDF for NLO simulations [41]. All of the simulations have been performed using the dynamical factorization and renormalization scales as implemented in the `MadGraph5` version `MG5_aMC_v2_5_3` original tune.

We have performed the selection of events defined at the end of Sec. III A. We have checked the sensitivity of the selection cuts on the event reconstruction parameters and found that the jet veto depends quite sensitively on the jet clustering algorithm. In particular, it becomes less efficient for narrower jets.

In Table II we show how the signal and the main backgrounds behave upon detector effects and selection cuts for the above-described event reconstruction and selection. Using the fifth and last columns, one can

⁵We note that in a five-flavor PDF scheme the QCD corrections to both processes are identical, the difference being purely in the PDFs. We also note that at NLO the signal and the $tW(b)$ background mix with the LO $t\bar{t}$ process and strategies exist for separating these with small remaining interference [34]. Unfortunately, exact NLO results and simulations of our signal are at present not publicly available and go beyond the scope of our work.

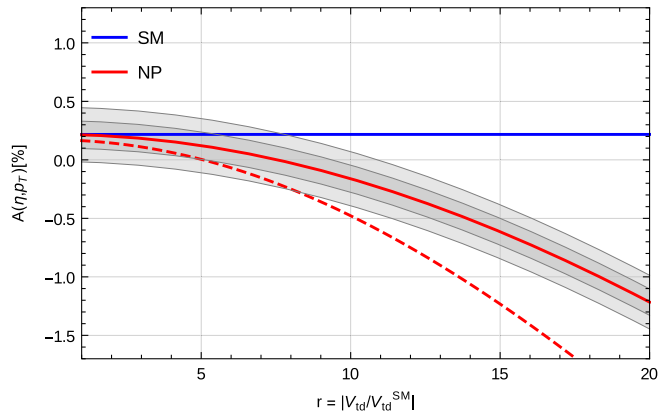


FIG. 5. Expected value of the asymmetry $A(\eta, p_T)$ (solid red) as function of the NP parameter $r = |V_{td}/V_{td}^{\text{SM}}|$. The shaded area represents statistical (darker)+assumed systematic (lighter) uncertainties ($\pm 1\sigma$) with the event selection indicated in the text at the prospective LHC luminosity of $L = 3000 \text{ fb}^{-1}$. The blue line represents the SM value of the asymmetry, which is mainly due to NLO QCD effects in $t\bar{t}$. Also shown (in dashed red) is an estimation of the asymmetry assuming a reduction of the dominant $t\bar{t}$ background by half (see the text for details).

visualize the importance of each contribution to the denominator and numerator of the asymmetry defined in Eq. (5), respectively. In Fig. 5 we plot the resulting charge asymmetry $A(\eta, p_T)$ defined in Eq. (5) with all of the detector-level simulations included. One can see that the $t\bar{t}$ asymmetry dominates for $r = \mathcal{O}(1)$ (close to the SM), but as r increases the negative contribution from the signal starts to dominate.

To quantify the versatility of the proposed charge asymmetry we have studied the prospective experimental reach in the NP parameter r by computing the difference of $A(\eta, p_T)$ to its SM expectation in units of the uncertainty. In addition to the statistical uncertainty we have included an estimation for the systematic uncertainty $\Delta_{\text{sys}} = 0.2\%$, based on a similar analysis in the dilepton charge asymmetry performed by the CMS Collaboration in Refs. [42,43] and the expected usual improvement in the knowledge of the detector and other systematic effects with increasing luminosity. In our analysis, Δ_{sys} acts as an overall estimation of all of the systematic uncertainties. By adding statistical and systematic uncertainties in quadrature, we define the significance as

$$\text{significance} = \frac{|A(\eta, p_T) - A(\eta, p_T)^{\text{SM}}|}{\sqrt{(N^+ + N^-)^{-1} + \Delta_{\text{sys}}^2}}. \quad (9)$$

In Fig. 6 we plot contours of expected significance in measuring $A(\eta, p_T)$ as a function of r and the luminosity. In order to further differentiate between the small signal and the overwhelming $t\bar{t}$ background, existing experimental analyses [27–29] of tW -associated production at the

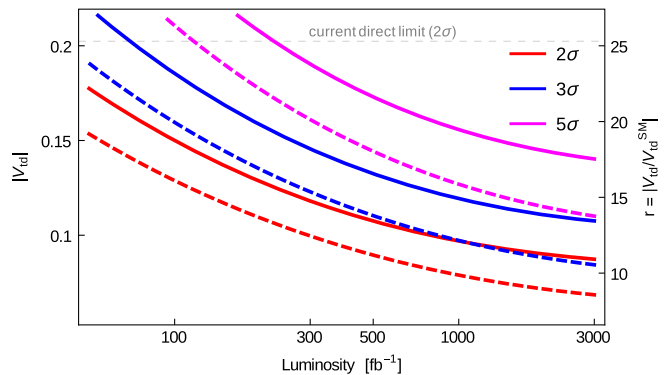


FIG. 6. Contour lines for the 2σ , 3σ , and 5σ measurement of $|V_{td}|$ parametrized as a function of $r = |V_{td}/V_{td}^{\text{SM}}|$ and the LHC luminosity. Dashed lines correspond to the estimation of the same analysis assuming a further reduction of the $t\bar{t}$ background by half (see text for details).

LHC—in addition to basic selection cuts similar to the ones described above—employ more elaborate multivariate techniques, such as boosted decision trees or neural networks. With the rapid development of machine learning, these methods are expected to be further refined in the near future and also extremely useful for the processes and observables studied here. As a rough estimation, and motivated by Ref. [27], we include in Fig. 6 (as a red dashed line) an estimation of the significance for the case where the $t\bar{t}$ background could be reduced by a further factor of $1/2$ with negligible effect on the signal.

We observe that in using the proposed charge asymmetry $A(\eta, p_T)$ in the leptonic tW final state, an improvement in the direct bound on $|V_{td}|$ (r) compared to existing constraints is possible already with the existing LHC data set. Furthermore, values of $r < 10$ could be directly accessible at the (HL) LHC, improving the existing best direct constraints by roughly a factor of 3. A further significant improvement would however require a reduction of systematic uncertainties below the per-mille level.

V. CONCLUSIONS

The CKM elements V_{td} and V_{ts} are fundamental parameters of the SM governing flavor conversion in the top sector. Their determination through direct measurements is a difficult task that requires processes with on-shell top quarks. We have proposed an observable that can test $|V_{td}|$ to $\mathcal{O}(10^{-1})$ in the creation of tW at the LHC. Selecting a final state with $\ell^+ \ell^- b p_T^{\text{miss}}$, we have defined a charge asymmetry using the variables η and p_T of the leptons that is sensitive to $|V_{td}|$. We have studied and characterized the signal and main backgrounds at the parton level, as well as by using simulations up to the (parametric) detector level. We have shown that, although the backgrounds have overwhelming production cross sections, they are highly symmetric and an asymmetric signal can

eventually emerge. We have computed the asymmetry as a function of $|V_{td}|$, and determined the prospective reach of the LHC as a function of the luminosity. We have shown that the current bound on the direct determination of $|V_{td}|$ can be surpassed with the existing LHC data set, and that with 3000 fb^{-1} it could be possible to exclude $|V_{td}| \gtrsim 0.1$ at the 2σ level.

The dominant $t\bar{t}$ background, although being charge symmetric at leading order, strongly suppresses the asymmetry by giving a large contribution to its denominator. A crucial improvement upon our cut-based approach would therefore be to further reduce this background while preserving the signal (using, e.g., multivariate or machine-learning techniques). As an example, we have shown in Fig. 6 that, by lowering $t\bar{t}$ by a factor 2, it would be possible to exclude $|V_{td}| \gtrsim 0.1$ already with 600 fb^{-1} of luminosity. Finally, a further significant reduction in systematic uncertainties below our current estimate of 0.2% could allow the (HL) LHC to eventually probe values as low as $|V_{td}| \sim 0.06$. In fact, taking as reference the current $t\bar{t}$ charge asymmetry systematics in the dileptonic final state [42], we see that the main sources of systematics come from the uncertainty due to the factorization and renormalization scale variations in the theoretical $t\bar{t}$ prediction, and due to the limited number of events in the MC@NLO Monte Carlo sample, both contribute 0.2%. The latter would not be a problem in the future,

whereas the former would require the use of improved theoretical predictions.

We have also studied a number of alternative definitions of the charge asymmetry, including asymmetries only in $\eta(\ell)$, as well as the implementation of additional cuts that could increase their size. We found that in all of the cases the total uncertainty increases, and the significance is at best comparable with the original one.

Finally, we comment on other processes that could also give valuable information for the direct determination of V_{tq} at the LHC. For example, kinematical distributions in t -channel single top production could also be used to probe V_{ts} (and V_{td}) suppressed contributions [23]. However, a much less explored example is $pp \rightarrow W^+W^-$, which is sensitive to V_{td} and V_{ts} and can be studied at the LHC. It can be complementary to the observables proposed in this paper and in the existing literature and certainly deserves a detailed study.

ACKNOWLEDGMENTS

J. F. K. acknowledges the financial support from the Slovenian Research Agency (research core funding No. P1-0035 and J1-8137). This work was partially supported by the Argentinian ANPCyT PICT 2013-2266 and by the cooperation agreement MHEST-MINCyT SLO-14-01, ARRS BI-AR/15-17-001, between Slovenia and Argentina.

-
- [1] C. Patrignani *et al.* (Particle Data Group), *Chin. Phys. C* **40**, 100001 (2016).
 - [2] J. C. Hardy and I. S. Towner, *Phys. Rev. C* **91**, 025501 (2015).
 - [3] D. Pocaric *et al.*, *Phys. Rev. Lett.* **93**, 181803 (2004).
 - [4] N. Cabibbo, E. C. Swallow, and R. Winston, *Annu. Rev. Nucl. Part. Sci.* **53**, 39 (2003).
 - [5] J. P. Lees *et al.* (BABAR Collaboration), *Phys. Rev. D* **91**, 052022 (2015).
 - [6] A. Zupanc *et al.* (Belle Collaboration), *J. High Energy Phys.* **09** (2013) 139.
 - [7] J. P. Lees *et al.* (BABAR Collaboration), *Phys. Rev. D* **95**, 072001 (2017).
 - [8] M. Neubert, *Phys. Rev. D* **49**, 3392 (1994).
 - [9] R. Aaij *et al.* (LHCb Collaboration), *New J. Phys.* **15**, 053021 (2013).
 - [10] J. Charles *et al.*, *Phys. Rev. D* **91**, 073007 (2015).
 - [11] J. A. Aguilar-Saavedra, R. Benbrik, S. Heinemeyer, and M. Prez-Victoria, *Phys. Rev. D* **88**, 094010 (2013).
 - [12] W. Buchmuller and D. Wyler, *Nucl. Phys.* **B268**, 621 (1986).
 - [13] B. Grzadkowski, M. Iskrzynski, M. Misiak, and J. Rosiek, *J. High Energy Phys.* **10** (2010) 085.
 - [14] S. Fajfer, A. Greljo, J. F. Kamenik, and I. Mustac, *J. High Energy Phys.* **07** (2013) 155.
 - [15] V. Khachatryan *et al.* (CMS Collaboration), *Phys. Lett. B* **736**, 33 (2014).
 - [16] M. Aaboud *et al.* (ATLAS Collaboration), *J. High Energy Phys.* **04** (2017) 086.
 - [17] M. Aaboud *et al.* (ATLAS Collaboration), *Eur. Phys. J. C* **77**, 531 (2017).
 - [18] A. M. Sirunyan *et al.* (CMS Collaboration), *Phys. Lett. B* **772**, 752 (2017).
 - [19] J. M. Campbell, R. Frederix, F. Maltoni, and F. Tramontano, *Phys. Rev. Lett.* **102**, 182003 (2009).
 - [20] P. Kant, O. M. Kind, T. Kintscher, T. Lohse, T. Martini, S. Mölbitz, P. Rieck, and P. Uwer, *Comput. Phys. Commun.* **191**, 74 (2015).
 - [21] M. Brucherseifer, F. Caola, and K. Melnikov, *Phys. Lett. B* **736**, 58 (2014).
 - [22] E. L. Berger, J. Gao, C. P. Yuan, and H. X. Zhu, *Phys. Rev. D* **94**, 071501 (2016).
 - [23] H. Lacker, A. Menzel, F. Spettel, D. Hirschbuhl, J. Luck, F. Maltoni, W. Wagner, and M. Zaro, *Eur. Phys. J. C* **72**, 2048 (2012).
 - [24] T. Lagouri, in *Proceedings of the 7th International Workshop on the CKM Unitarity Triangle (CKM 2012)*, Cincinnati, Ohio, USA, 2012 (to be published), arXiv:1212.0013.

- [25] T. M. P. Tait and C. P. Yuan, *Phys. Rev. D* **63**, 014018 (2000).
- [26] J. Alwall, R. Frederix, S. Frixione, V. Hirschi, F. Maltoni, O. Mattelaer, H. S. Shao, T. Stelzer, P. Torrielli, and M. Zaro, *J. High Energy Phys.* **07** (2014) 079.
- [27] S. Chatrchyan *et al.* (CMS Collaboration), *Phys. Rev. Lett.* **112**, 231802 (2014).
- [28] G. Aad *et al.* (ATLAS Collaboration), *J. High Energy Phys.* **01** (2016) 064.
- [29] M. Aaboud *et al.* (ATLAS Collaboration), [arXiv:1612.07231](https://arxiv.org/abs/1612.07231).
- [30] S. Frixione, E. Laenen, P. Motylinski, B. R. Webber, and C. D. White, *J. High Energy Phys.* **07** (2008) 029.
- [31] E. Alvarez, D. A. Faroughy, J. F. Kamenik, R. Morales, and A. Szykman, *Nucl. Phys.* **B915**, 19 (2017).
- [32] F. Maltoni, G. Ridolfi, and M. Ubiali, *J. High Energy Phys.* **07** (2012) 022; **04** (2013) 95.
- [33] N. Kidonakis, in *Proceedings of the 15th International Workshop on Deep-Inelastic Scattering and Related Subjects (DIS 2007), Munich, Germany, April 16–20, 2007*, edited by G. Grindhammer and K. Sachs (DESY, Hamburg, 2007), p. 443.
- [34] C. D. White, S. Frixione, E. Laenen, and F. Maltoni, *J. High Energy Phys.* **11** (2009) 074.
- [35] J. Bellm *et al.*, *Eur. Phys. J. C* **76**, 196 (2016).
- [36] M. Bahr *et al.*, *Eur. Phys. J. C* **58**, 639 (2008).
- [37] T. Sjöstrand, S. Ask, J. R. Christiansen, R. Corke, N. Desai, P. Ilten, S. Mrenna, S. Prestel, C. O. Rasmussen, and P. Z. Skands, *Comput. Phys. Commun.* **191**, 159 (2015).
- [38] T. Sjostrand, S. Mrenna, and P. Z. Skands, *J. High Energy Phys.* **05** (2006) 026.
- [39] J. de Favereau, C. Delaere, P. Demin, A. Giammanco, V. Lemaître, A. Mertens, and M. Selvaggi (DELPHES 3 Collaboration), *J. High Energy Phys.* **02** (2014) 057.
- [40] A. Collaboration, Technical Report, CERN, Geneva (2015), <https://cds.cern.ch/record/2037697>.
- [41] A. Buckley, J. Ferrando, S. Lloyd, K. Nordström, B. Page, M. Rfenacht, M. Schnherr, and G. Watt, *Eur. Phys. J. C* **75**, 132 (2015).
- [42] V. Khachatryan *et al.* (CMS Collaboration), *Phys. Lett. B* **760**, 365 (2016).
- [43] M. Naseri (ATLAS and CMS Collaborations), in *Proceedings of the 9th International Workshop on Top Quark Physics (TOP 2016), Olomouc, Czech Republic, 2016* (to be published), [arXiv:1703.03558](https://arxiv.org/abs/1703.03558).